Molecular Biology Reports (2024) 51:832
https://doi.org/10.1007/s11033-024-09764-3

ORIGINAL ARTICLE

Ruxolitinib-loaded poly-ε-caprolactone (PCL) nanoparticles inhibit JAK2/STAT5 signaling in BT474 breast cancer cells by downregulating Bcl-2 and Mcl-1

Esin Guvenir Celik[1,2] · **Onur Eroglu**[1]

Received: 18 April 2024 / Accepted: 27 June 2024 / Published online: 22 July 2024

Abstract

Background JAK/STAT signaling plays an important role in regulating cell proliferation. Reducing proliferation and inducing cell death with gene-specific inhibitors such as ruxolitinib, Receptor tyrosine kinases (RTK) inhibitor targeting JAK1/2, are therapeutic approaches. The use of nanoparticles can reduce the toxicity and side effects of drugs, as they act directly on cancer cells and can selectively increase drug accumulation in tumor cells. Poly-ε-caprolactone (PCL) is a polymer that is frequently used in drug development. In this study, Rux-PCL-NPs were synthesized to increase the effectiveness of ruxolitinib. In addition, this study aimed to determine the effect of Rux-PCL-NPs on JAK/STAT signaling and apoptotic cell death.

Methods and results Rux-PCL-NPs were synthesized by nanoprecipitation. The Rux-PCL-NPs had a spherical and mean particle size of 219 ± 88.66 nm and a zeta potential of 0.471 ± 0.453 mV. In vitro cytotoxicity and antiproliferative effects were determined by MTT and soft agar colony formation assays, respectively. The effects of ruxolitinib, PCL-NPs, and Rux-PCL-NPs on apoptosis and the JAK/STAT pathway in cells were examined by western blot analysis. PCL-NPs did not have a toxic effect on the cells. The IC_{50} value of Rux-PCL-NPs was decreased 50-fold compared to that of ruxolitinib. Rux-PCL-NPs promoted cell death by downregulating JAK2 and STAT5, thereby inhibiting the JAK/STAT pathway.

Conclusions Our results revealed that Rux-PCL-NPs, which increased the efficacy of ruxolitinib, regulated apoptosis and the JAK2/STAT5 pathway.

Keywords BT474 · Ruxolitinib · Poly-ε-caprolactone · Ruxolitinib-loaded poly-ε-caprolactone nanoparticles · JAK/STAT

Introduction

Breast cancer is the most common cancer diagnosed in women around the world [1]. The nuclear receptor superfamily includes estrogen receptors (ERs) and progesterone receptors (PRs). In mammary gland cells, ER/PR dysregulation contributes to carcinogenesis [1]. The PR and ER are prognostic markers for breast cancer and predictors of treatment response [2]. In most hormonal therapies, androgen-to-estrogen conversion is inhibited by blocking ER activity and aromatase activity [2]. Unfortunately, some patients develop resistance to endocrine therapy. The identification of new targets in resistant tumors is essential for the development of new therapeutic options for patients. It may be possible to develop new treatments for breast cancer by studying alternative cancer-associated signaling pathways, such as the Janus kinase (JAK) signal transducer and activator of transcription (STAT) signaling pathway.

In breast cancer, JAK/STAT signaling is constitutively active and regulates chemotherapy resistance [3]. There appears to be promise in treating breast cancer with drugs targeting different components of this pathway. The RTK inhibitor ruxolitinib suppresses JAK/STAT signaling by targeting JAK1/JAK2 [4]. This drug has been approved for the treatment of patients with polycythemia vera who fail

✉ Esin Guvenir Celik
esin.guvenir@bilecik.edu.tr

[1] Department of Molecular Biology and Genetics, Faculty of Science, Bilecik Seyh Edebali University, Bilecik, Turkey

[2] Department of Molecular Biology and Genetics, Institute of Graduate Education, Bilecik Şeyh Edebali University, Bilecik, Turkey

to respond to or are intolerant to hydroxyurea and those with intermediate and high-risk myelofibrosis. Several side effects have been reported, including anemia, leukopenia, thrombocytopenia, dizziness, headaches, and bruising [4]. Systemic side effects such as rapid dissolution of ruxolitinib in the blood have also been reported [5]. The numerous side effects of ruxolitinib on cells and patients documented in the literature has revealed the need to minimize the side effects of ruxolitinib and increase its effectiveness. At present, it is thought that these disadvantages can be eliminated by synthesizing a nanoform of the drug with nanoparticles, which can directly target cancer cells more effectively and selectively increase drug accumulation in these cells while reducing the toxicity and side effects of drugs.

Nanoparticles are drug carrier systems that target therapeutic genes without damaging normal cells and are used to reduce high doses of chemotherapeutic drugs to cancer cells [6]. Nanoparticles (NPs) are thought to be an important tool for reducing the toxicity and side effects of drugs, as they can directly target cancer cells and selectively increase drug accumulation in these cells, thus increasing the anticancer effects of drugs [7, 8]. Polymeric nanoparticles (PNPs) are a class of nanoparticles in which different polymers encapsulate a drug. These polymeric nanoparticles are used to target specific cancer cells or tissues by increasing the stability of the drug by binding to its ligand, which has an affinity for that cell, and they provide advantages due to their biocompatibility [8]. Poly-ε-caprolactone (PCL) is a highly hydrophobic and biodegradable polymer with a synthetic semicrystalline structure. This polymer degrades slowly in the physiological environment and does not cause the accumulation of toxic metabolites. PCL is widely used in drug development because of its biocompatibility and biodegradability. It can facilitate drug release through long-term degradation [9].

In the literature, there are several studies on PCL nanoparticles being loaded with certain drugs, such as paclitaxel [10], quercetin [11], irinotecan [12], 5-fluorouracil [13], cefotaxime [14], and atorvastatin calcium [15]. In the literature, there are two studies on ruxolitinib-loaded nanoparticles: gold-coated nanoparticles loaded with ruxolitinib [5] and a topical Emulgel containing ruxolitinib nanoliposomes [16]. In this study, ruxolitinib-loaded PCL nanoparticles were synthesized for the first time using a nanoprecipitation technique.

First, this study aimed to minimize the toxicity of ruxolitinib in its free form to cells and ensure that drug effectively reaches the cells. Second, this study aimed to increase the effectiveness of ruxolitinib in BT474 (ER+, PR+, HER2+) cells by synthesizing Rux-PCL-NPs. Third, we aimed to understand the effect of Rux-PCL-NPs on JAK/STAT signaling and apoptotic cell death.

Materials and methods

Drugs, chemicals and antibodies

Ruxolitinib was purchased from MedChemExpress (USA). Rabbit antibodies against β-actin (CST-4970), PARP (CST-9532), Caspase-9 (CST-9508), Caspase-7 (CST-12,827), and Caspase-3 (CST-9662) (1:1000 dilution) were purchased from Cell Signaling Technology (CST, Danvers, MA, USA). Mouse antibodies against JAK2 (sc-390,539), STAT5 (sc-74,442), STAT3 (sc-8019), Caspase-8 (sc-56,070), Bax (sc-20,067), Bcl-2 (sc-7382), and c-Myc (sc-40) (1:500 dilution) were purchased from Santa Cruz Biotechnology (sc, Oregon, USA). HRP-conjugated anti-rabbit and anti-mouse secondary antibodies (1:5000 dilution) were purchased from CST.

Synthesis of PCL, blank and drug-loaded PCL nanoparticles

Synthesis of PCL nanoparticle

PCL nanoparticles were prepared using the nanoprecipitation method. One hundred milligrams of PCL was dissolved in 25 ml of acetone. This organic solution was added dropwise to 75 ml of dH_2O (cold) aqueous solution containing 0.1% (w/v) acetic acid and 0.03% (w/v) Tween 80 in a magnetic stirrer in an ice bath. The resulting suspension was centrifuged at 16,000 × g for 75 min at 4 °C. The supernatant was removed. The pellet was frozen at -20 °C for 24 h and lyophilized for 24 h (Biobase, BK-FD10S) [17].

Synthesis of ruxolitinib-noaded PCL nanoparticles

Ruxolitinib-loaded PCL nanoparticles (Rux-PCL-NPs) were prepared using the nanoprecipitation method. PCL (10 mg) was dissolved in 5 ml of acetone. Then, ruxolitinib (1 mg) was dissolved in 1 ml of DMSO, added to the mixture, and mixed thoroughly. This organic solution was added dropwise on a magnetic stirrer to 20 ml of dH_2O (cold) containing 0.03% Tween 80 and stirred at room temperature for 1 night to allow the organic solvent to evaporate completely and promote the precipitation of the nanoparticles. The resulting suspension was centrifuged at 16,000 × g for 75 min at 4 °C. The supernatant was removed. The pellet was frozen at -20 °C for 24 h and lyophilized for 24 h (Biobase, BK-FD10S). The samples were stored at 4 °C until use. Blank NPs (PCL nanoparticles) were used as a control [18, 19].

Characterization of nanoparticles

Zeta potential and particle size measurement

The average size and zeta potential of the Rux-PCL-NPs were measured with a Zetasizer (Malvern, NANO-ZS). Fifty microliters of the nanoparticle solution was added to 950 µl of ddH_2O, and 1 ml of the solution was prepared and read at 25 °C. The polydispersity index and zeta potential were analyzed in three groups to obtain average values for the standard deviation and mean size [19].

Morphological analysis of drug-loaded PCL nanoparticles

The size and surface morphology of the ruxolitinib-loaded PCL nanoparticles were examined by scanning electron microscopy (SEM). Lyophilized Rux-PCL-NPs were coated with gold for 1 min after being dropped onto a Stub plate with carbon tape attached. Then, a scanning electron microscope (ZEISS/Supra 40 VP)was used to determine their sizes and morphologies [10].

Assessment of encapsulation efficiency and drug loading capacity

The encapsulation of ruxolitinib in a biocompatible PCL polymer was achieved via a nanoencapsulation method. PCL nanoparticles encapsulated with ruxolitinib were developed by the nanoprecipitation technique. After centrifuging the samples at 16,000 rpm for 45 minutes, the amount of drug-containing nanoparticles was determined. The separation of free nanoparticles in the supernatant was ensured. The amount of unencapsulated free ruxolitinib was determined using the nanoparticle supernatant as a blank in a UV spectrophotometer at a wavelength of 230 nm. The encapsulation efficiency (EE) and drug loading capacity (DL) of the Rux-PCL-NPs were determined via the following formula [18]:

$$EE\,(\%) = \left(\frac{\text{Weight of Rux in the NP}}{\text{Initial weight of Rux used}}\right) \times 100$$

$$DL\,(\%) = \left(\frac{\text{Weight of Rux in the NP}}{\text{Total weight of NP}}\right) \times 100$$

In vitro ruxolitinib release

The in vitro drug release of PCL nanoparticles containing the active ingredients of ruxolitinib was determined by a dialysis membrane technique. The dialysis membrane (MWCO: 14.000 Da) was activated with 70% EtOH. PCL nanoparticle suspensions containing ruxolitinib active ingredients were transferred to dialysis membranes, placed in 75 ml of phosphate-buffered saline (PBS) (pH 7.4) and incubated at 37 °C and 200 rpm. After 0.5, 1, 2, 4, 8, 16, 24, 36, 48, 72, and 96 h, 2 ml of sample was replaced with PBS, and the samples were incubated at the same volume and temperature. The samples were measured with a UV spectrophotometer at 230 nm. The amount of drug released was determined for each measurement hour by drawing a graph for each formulation with the measured absorbance values [10].

Investigation of the anticancer effect of Rux-PCL-NPs

Cell Culture

BT474 cells were incubated in RPMI medium supplemented with 1% NEAA, 0.1% insulin, 1% penicillin/streptomycin, and 20% heat-inactivated fetal bovine serum (FBS) in 37 °C incubators containing 5% CO_2 (Memmert CO_2 Incubator, INCO153med, Germany).

In vitro cytotoxicity

Three-(4.5-dimethylthiazol-2-yl)-2.5-diphenyl-2 H-tetrazolium-bromide (MTT) assays were used to examine the viability of BT474 breast cancer cells treated with ruxolitinib and Rux-PCL-NPs at different concentrations. BT474 cells were seeded at 1×10^4 in each well of a 96-well Petri dish. After attaching the cells to the Petri dish, Ruxolitinib and the Ruxolitinib-loaded PCL nanoparticles were applied for 48 h. To each well, 10 µl of MTT was added, and the plate was then incubated at 37 °C for 4 h. After incubation for 5 minutes in the dark, the medium with the MTT reagent was removed and 100 µl of DMSO was added to the wells. The absorbance values were measured at dual wavelengths of 570 nm and 655 nm on an ELISA reader (Multiskan™ FC Microplate Photometer, Thermo Fisher Scientific, Multiskan FC China).

Soft agar colony formation analysis

The soft agar colony formation test was used to observe the ability of the cells to grow in an environment where their adhesion to the surface was prevented. Six-well Petri dishes were covered with previously prepared and autoclaved 2X media containing 0.5% agarose solution and 20% FBS at a 1:1 ratio. BT474 cells were seeded as 2.5×10^3 cells in Petri dishes covered with 2× media, 0.3% agarose, and 0.5% agarose at a cell ratio of 1:1. The cells were incubated

with ruxolitinib and Rux-PCL-NPs at the determined concentrations for 15 days and grown in 37 °C incubators containing 5% CO_2. The cells were cultured by removing the upper media and adding new media every 2 days. The colonies were examined under an inverted microscope (Nikon Eclipse TS100-F) at 100× magnification and stained with 0.5 ml of 0.005% crystal violet for 20 minutes.

Western blotting

Cells were treated with 0.3267 µM Rux-PCL-NPs and 50 µM ruxolitinib for 48 h. After all the samples were washed with 1× PBS, they were centrifuged at 13,200 rpm for 2 minutes. Cells were lysed on ice for 5 minutes with radioimmunoprecipitation assay (RIPA) solution (CST-9806). After the cells were lysed, they were shaken at room temperature for 20 minutes. After centrifuging the cells for 15 min at 13,200 rpm, the supernatant was collected. A semidry transfer system (Hoefer) was used to transfer the protein lysates (50 µg), as determined by the Bradford protein assay, to PVDF membranes (Merck Millipore). Primary and secondary antibodies were incubated at 4 °C overnight. After the washing steps, the protein expression levels of JAK2 (sc-390,539), STAT3 (sc-8019), STAT5 (sc-74,442), PARP (CST-9532), Caspase 8 (sc-56,070), Caspase 9 (CST-9508), Caspase 7 (CST-12,827), Caspase 3 (CST-9662), β-actin (CST-4970), Bax (sc-20,067), c-Myc (sc-40), and Bcl-2 (sc-7382) were analyzed via enhanced chemiluminescence (ECL, Thermo Fisher Scientific) in a Syngene G: Box Chemi XRQ system.

Statistical analysis

Each experiment was analyzed using one-way analysis of variance (ANOVA) with GraphPad Prism 9.0.0. The graph error bars represent the standard deviations (SDs), which were calculated from at least three independent experiments. Using ImageJ, SD values were calculated for the fluorescence intensities of proteins obtained from western blotting. The mean value of three measurements was used for each protein. The relative expression level of each protein was calculated by dividing the value of the protein by the value of β-actin. In this study, statistical significance was defined as * $P<0.05$; ** $P<0.01$; ***$P<0.001$; and **** $P<0.0001$.

Results

Synthesis and characterization of PCL and ruxolitinib-loaded PCL nanoparticles

PCL nanoparticles (PCL-NPs) and ruxolitinib-loaded PCL nanoparticles (Rux-PCL-NPs) were synthesized by nanoprecipitation, and the samples were stored at -20 °C [18, 19]. The average size, zeta potential, and PDI values of pure ruxolitinib and the synthesized PCL-NPs and Rux-PCL-NPs were determined via a Zetasizer instrument. The average sizes of ruxolitinib, PCL-NPs, and Rux-PCL-NPs were 564.4641 ± 25.4505 nm, 159.4 ± 74.72 nm, and 219 ± 88.66 nm, respectively (Table 1). The zeta potentials of ruxolitinib, PCL-NPs, and Rux-PCL-NPs were − 44.6 ± 6.19 mV, -0.372 ± 0.449 mV, and 0.471 ± 0.453, respectively (Table 1). The polydispersity index (PDI) values of ruxolitinib, PCL-NPs, and Rux-PCL-NPs were 0.696, 0.756 ± 0.172, and 0.669 ± 0.245, respectively (Table 1). The %EE and %DL values of the Rux-PCL-NPs were 61% and 6.1%, respectively (Table 1).

Morphological characterization of PCL and ruxolitinib-loaded PCL nanoparticles

The surface morphology of the Rux-PCL-NPs was determined by SEM. The molecular size of ruxolitinib decreased with increasing encapsulation of PCL (Fig. 1a and b). The size of the Rux-PCL-NPs varied between 97 and 101 nm.

In vitro release

In vitro drug release of ruxolitinib from the synthesized PCL nanoparticles was carried out using the dialysis membrane technique (Fig. 2). It was determined that 51% of the ruxolitinib was released from the PCL nanoparticles in the first 24 h (Fig. 2). At the end of the 96th hour, 77% of the ruxolitinib was released (Fig. 2).

Table 1 Ruxolitinib payload, encapsulation efficiency, size, size distribution (polydispersity), and Zeta potential of the NPs at 25 °C. The results are expressed as the mean ± S.D. (n = 3)

Sample	Size (nm) (± SD)	Polydispersity (± S.D.)	Zeta potential (mV) (± SD)	Encapsulation efficiency (%)	Drug loading (%w/w)
Ruxolitinib	564.4641 ± 25.45057	0.696	-44.6 ± 6.19		
PCL-NPs	159.4 ± 74.72	0.756 ± 0.172	-0.372 ± 0.449		
Rux-PCL-NPs	219 ± 88.66	0.669 ± 0.245	0.471 ± 0.453	61	6.1

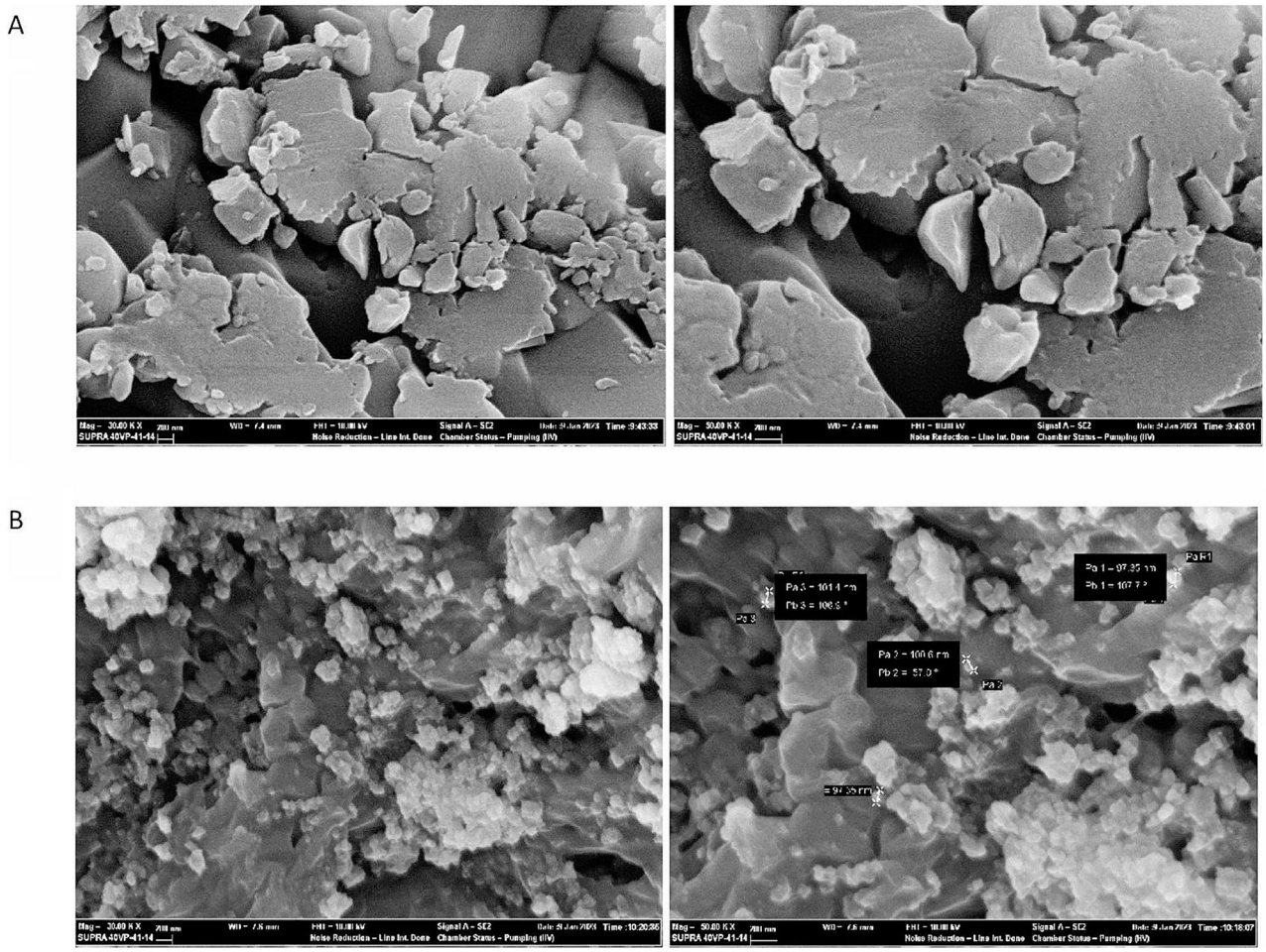

Fig. 1 Morphological structure of ruxolitinib (**A**) and synthesized Rux-PCL-NPs (**B**)

In vitro cytotoxicity of ruxolitinib and Rux-PCL-NPs

To determine the dose- and time-dependent in vitro cytotoxicity of ruxolitinib, PCL-NPs, and Rux-PCL-NPs in BT474 cells, 24-, 48-, and 72-hour MTT cell viability assays were performed (Fig. 3a, b and c). BT474 cells were treated with various concentrations of ruxolitinib (0–50 µM) [20, 21], PCL-NPs (0–2500 µM), or Rux-PCL-NPs (0–490 µM) for 24, 48, or 72 h. To determine whether the decrease in cell viability was due to ruxolitinib itself or the DMSO in which it was dissolved, DMSO was applied to the cells at a maximum final concentration of 0.1%. PCL-NP application had no toxic effect on the BT474 cells (Fig. 3b). Treatment with ruxolitinib or Rux-PCL-NPs for 24 h was not effective against BT474 breast cancer cells, and 72 h of ruxolitinib or Rux-PCL-NP treatment was toxic. Therefore, the experiments were continued with 48 h of ruxolitinib and Rux-PCL-NP treatment (Fig. 3c). The IC_{50} values of ruxolitinib, PCL-NPs, and Rux-PCL-NPs on BT474 cells were 50 µM, 1.6 µM, and 0.3267 µM, respectively (Table 2).

Effects of ruxolitinib and rux-PCL-NPs on colony formation

The ability of the cells to grow on soft agar surfaces where they were prevented from adhering to the surface was tested (Fig. 4). BT474 cells in the untreated control group and the DMSO-treated group exhibited similar sizes of colonies. PCL did not prevent colony formation in BT474 cells, but ruxolitinib and Rux-PCL-NPs significantly inhibited colony formation in BT474 cells.

Apoptosis is induced by Rux-PCL-NPs

Using western blotting, changes in the expression of proteins involved in the apoptotic pathway were examined in response to ruxolitinib, PCL-NPs, and Rux-PCL-NPs treatment. BT474 cells treated with ruxolitinib exhibited decreased expression of PARP, Caspase-3, Caspase-8, and Caspase-7 but not Caspase-9 (Fig. 5a). In BT474 cells, Rux-PCL-NPs treatment decreased PARP, Caspase-8, and

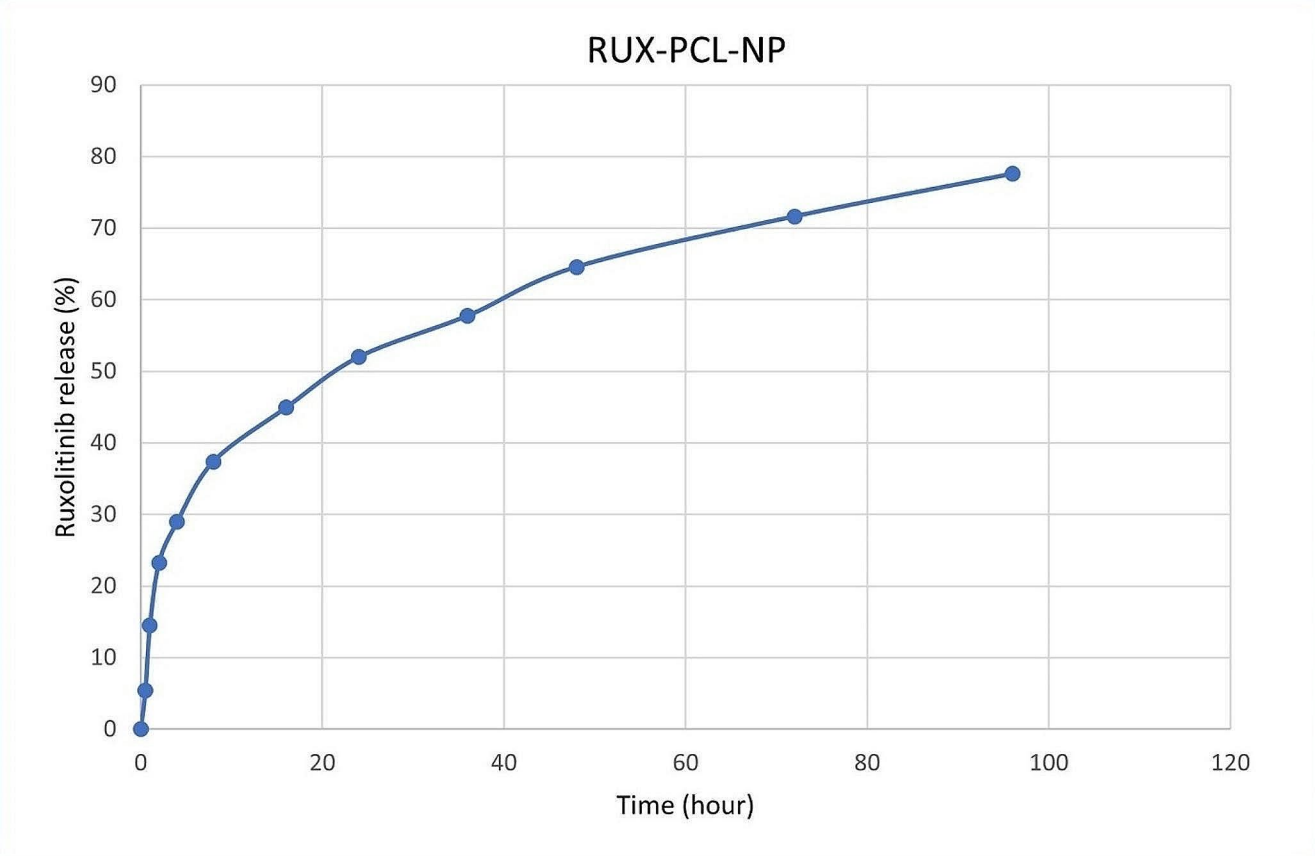

Fig. 2 Ruxolitinib release from PCL nanoparticles at 37 °C over 96 h

Caspase-3 expression, whereas Caspase-9 and Caspase-8 expression did not change (Fig. 5b).

The members of the Bcl-2 family play essential roles in regulating apoptosis by balancing pro- and antiapoptotic activities. The effects of ruxolitinib, PCL-NPs, and Rux-PCL-NPs on the apoptotic pathway were investigated by western blotting to determine the changes in the expression of the pro- and antiapoptotic proteins in BT474 cells (Fig. 5c and d). Treatment of BT474 cells with ruxolitinib increased the expression of Bax, a member of the proapoptotic Bcl-2 family, decreased the expression of Mcl-1 and Bcl-2, did not significantly change the expression of Bad, and increased the expression of c-Myc (Fig. 5c). The expression of Bcl-2 and Mcl-1 decreased with Rux-PCL-NP treatment in BT474 cells, and there was no change in the expression of Bad, Bax, or c-Myc (Fig. 5d).

Rux-PCL-NPs inhibit JAK2/STAT3 signaling

To investigate the effects of ruxolitinib, PCL-NPs, and Rux-PCL-NPs on JAK/STAT signaling, which is a cell survival pathway, in BT474 cells, changes in protein levels were determined by immunoblotting (Fig. 6a and b). Ruxolitinib reduced the expression of STAT5 and JAK2 in BT474 cells, while the expression of STAT3 did not change. STAT3 expression decreased with Rux-PCL-NP treatment in BT474 cells, but STAT5 and JAK2 expression did not significantly change.

Discussion

Breast cancer remains the most commonly diagnosed cancer in women [1]. Progesterone receptors (PRs) and estrogen receptors (ERs) belong to the nuclear receptor superfamily. In mammary gland cells, ER/PR dysregulation causes tumorigenesis, so these receptors are prognostic markers for breast cancer [1]. Additionally, ERs and PRs can be used to predict treatment response [2]. Because of the development of resistance to endocrine therapy in some patients, most hormonal therapies focus on blocking ER activity and inhibiting aromatase-mediated androgen-to-estrogen conversion [2]. There is a need for new therapeutic approaches to treat resistant tumors. It may be possible to develop a new treatment strategy for breast cancer by understanding the mechanism of alternative cancer-associated signaling pathways, such as the JAK/STAT signaling pathway.

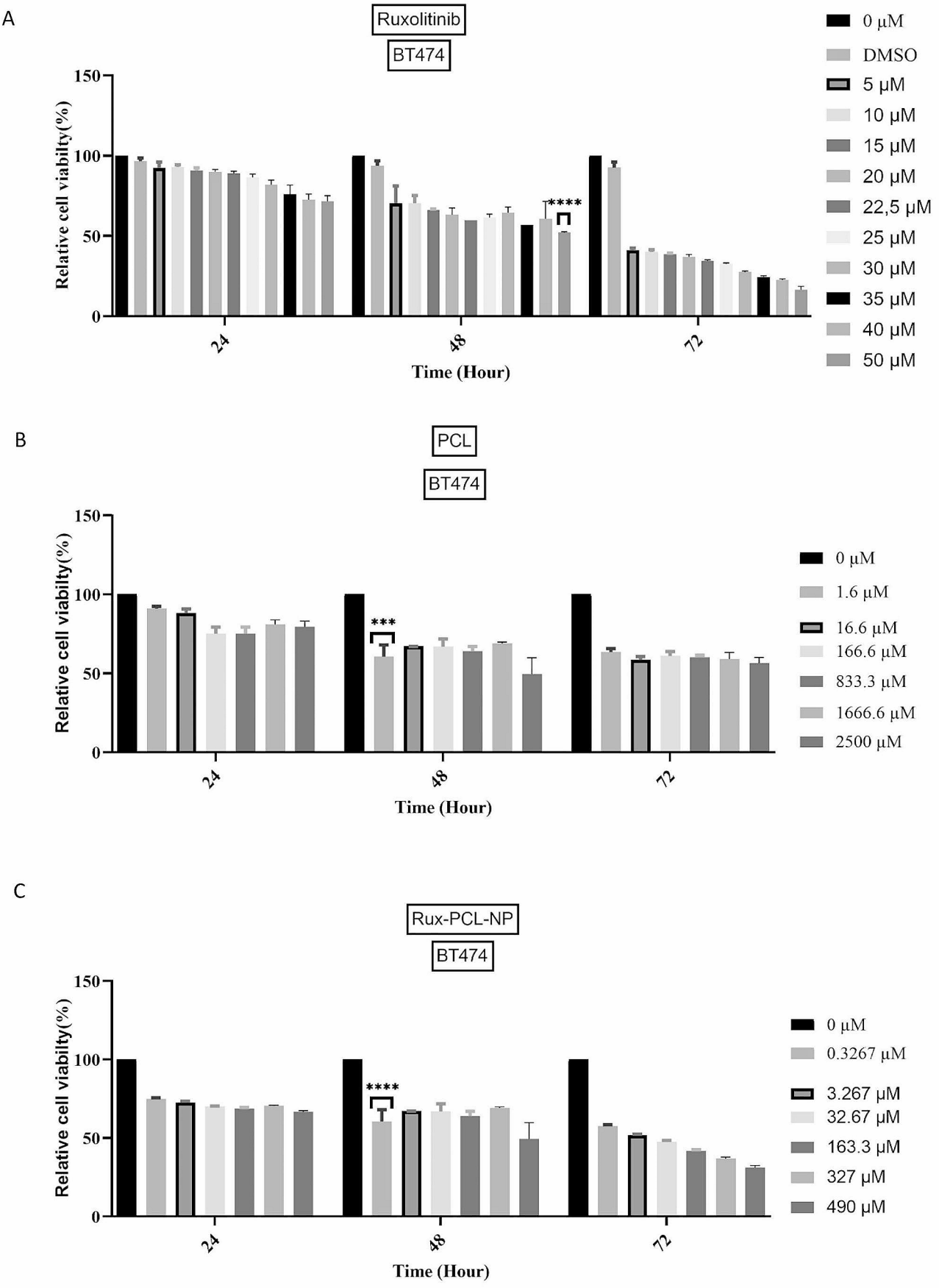
A
Ruxolitinib
BT474
Relative cell viabilty(%)
150
100
50
0
****
24
48
72
Time (Hour)
0 µM
DMSO
5 µM
10 µM
15 µM
20 µM
22,5 µM
25 µM
30 µM
35 µM
40 µM
50 µM
B
PCL
BT474
Relative cell viabilty(%)
150
100
50
0
***
24
48
72
Time (Hour)
0 µM
1.6 µM
16.6 µM
166.6 µM
833.3 µM
1666.6 µM
2500 µM
C
Rux-PCL-NP
BT474
Relative cell viabilty(%)
150
100
50
0
****
24
48
72
Time (Hour)
0 µM
0.3267 µM
3.267 µM
32.67 µM
163.3 µM
327 µM
490 µM

Fig. 3 Effect of ruxolitinib, PCL, and Rux-PCL-NPs on BT474 cell viability. In vitro cytotoxicity was determined by MTT assay after ruxolitinib (**a**), PCL (**b**), and Rux-PCL-NPs (**c**) treatment. Three independent experiments are indicated by the standard deviation (SD) values. Statistical differences were analyzed with one-way ANOVA and two-way ANOVA. *, **, *** and **** indicate $P < 0.05$, $P < 0.01$, $P < 0.001$, and $P < 0.0001$, respectively

Table 2 IC_{50} values determined by MTT assay after ruxolitinib, PCL-NP, and Rux-PCL-NP treatment in BT474 cells

	BT474
	IC_{50} Values
Ruxolitinib	50 µM
PCL	1.6 µM
Rux-PCL-NPs	0.3267 µM

Tumor cells inhibit apoptosis by decreasing caspase activity, disrupting the balance of proapoptotic and anti-apoptotic proteins, and disrupting death receptor signals [22]. In cancer cells, oncogenic mutations targeting signal transduction pathways and signaling proteins cause a loss of proliferation and survival control [23]. Continuous activation of cytoplasmic tyrosine kinases and oncogenic signal transmission accelerate cellular events such as tumor growth, transformation, angiogenesis, and invasion. RTKs regulate signaling pathways such as the JAK/STAT pathway. This pathway plays a crucial role in cell proliferation, angiogenesis, and metastasis. Ruxolitinib is an orally available receptor tyrosine kinase inhibitor that targets JAK1 and JAK2. It is approved for use in patients with myelofibrosis or polycythemia vera who are intolerant or inadequately responsive to hydroxyurea. The most commonly observed side effects are leukopenia, anemia, thrombocytopenia, headache, bruising, and dizziness [4]. Studies have revealed the need to minimize the side effects of ruxolitinib and increase its effectiveness [5]. At present, it is thought that its disadvantages can be circumvented by synthesizing the ruxolitinib-loaded nanoparticles, which can directly target cancer cells more effectively and selectively increase drug accumulation in these cells, thereby reducing the toxicity and side effects of the drug.

Due to the biodegradable and biocompatible features of PCL, it is frequently used in drug development studies because it can slowly release drugs for up to several months [9]. In the literature, studies related to paclitaxel- [10], quercetin- [11], irinotecan- [12], 5-fluorouracil- [13] and atorvastatin calcium- [15]loaded PCL nanoparticles have been reported. In the literature, there are only two studies on the ruxolitinib-loaded nanoparticles: gold-coated ruxolitinib-loaded nanoparticles [5] and a topical Emulgel containing ruxolitinib nanoliposomes [16]. In this study, ruxolitinib-loaded PCL nanoparticles were synthesized for the first time, and their effects on apoptosis and the JAT/STAT signaling pathway in triple-positive breast cancer cells were examined.

Particle size plays an important role in NP migration across the cell membrane and cellular uptake, as well as in determining the route of treatment. Especially in intravenous applications, the nanoparticle diameter should be below a certain size because it may obstruct blood capillaries. In contrast, smaller particles may have toxic effects because of their greater surface area [24]. Unal et al. [10] showed that the average size of the paclitaxel-loaded PCL nanoparticles they synthesized was between 199 and 383 nm and that the nanoparticle size may increase compared to that of blank nanoparticles due to paclitaxel settling on the nanoparticle surface. Similarly, in this study, the average sizes of the ruxolitinib, PCL-NPs, and Rux-PCL-NPs were 564.4641 ± 25.4505 nm, 159.4 ± 74.72 nm, and 219 ± 88.66 nm, respectively (Table 1). Studies have shown that drug-loaded nanoparticles can be larger than empty nanoparticles, and active transport makes carrier systems smaller than 500 nm more effective at delivering drugs to target tissues, especially tumor tissues [11]. According to our results, the particle size of the ruxolitinib-loaded PCL nanoparticles may have increased compared to that of the PCL-NPs due to the drugs settling on the nanoparticle surface.

The zeta potential plays an important role in determining the characteristics and stability of particles. Studies have shown that positively charged NPs have a high probability of interacting with the cell membrane because the

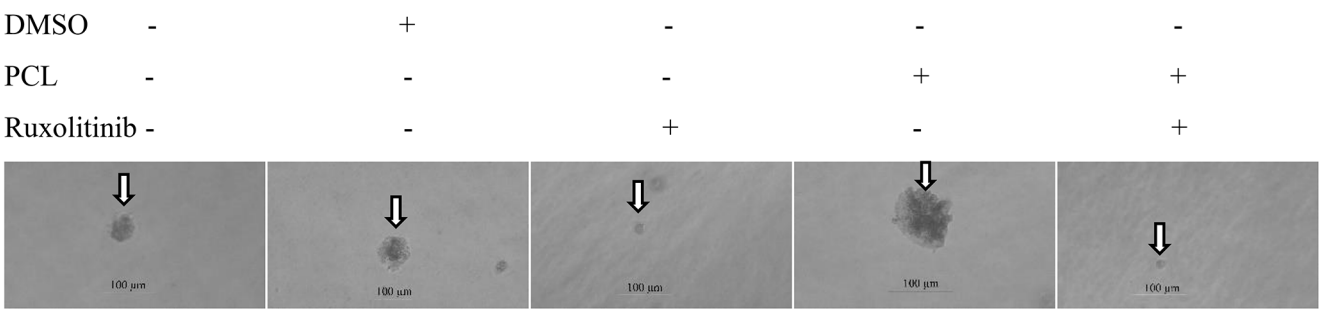

Fig. 4 Determination of the growth ability of ruxolitinib, PCL-NPs, and Rux-PCL-NPs in BT474 cells by a soft agar colony formation assay

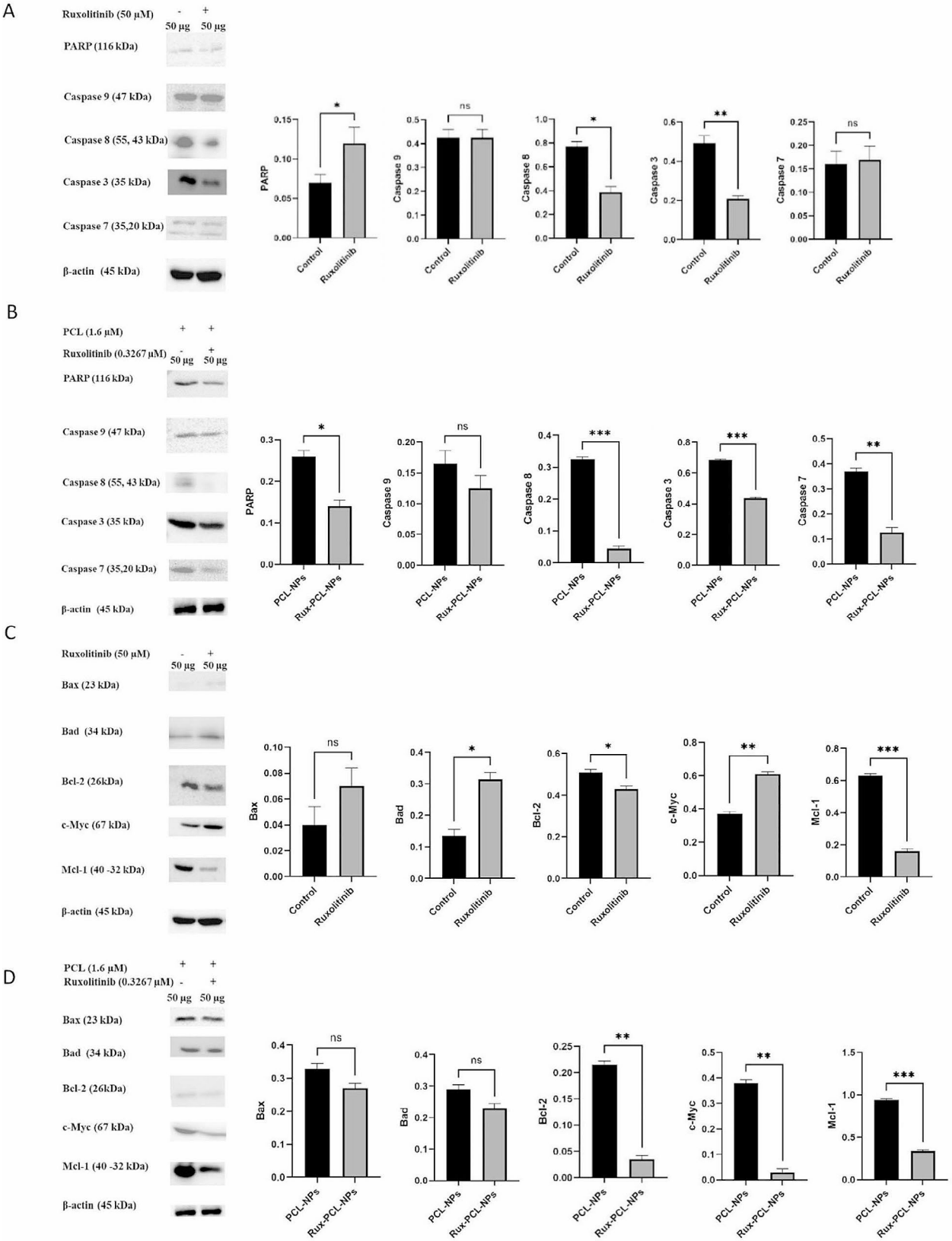

Fig. 5 Effects of ruxolitinib, PCL-NPs, and Rux-PCL-NPs on apoptosis. The effects of ruxolitinib (**a**), PCL-NPs (**b**), or Rux-PCL-NPs (**b**) on apoptosis and Bcl-2 family members (**c**, **d**) were examined by western blotting

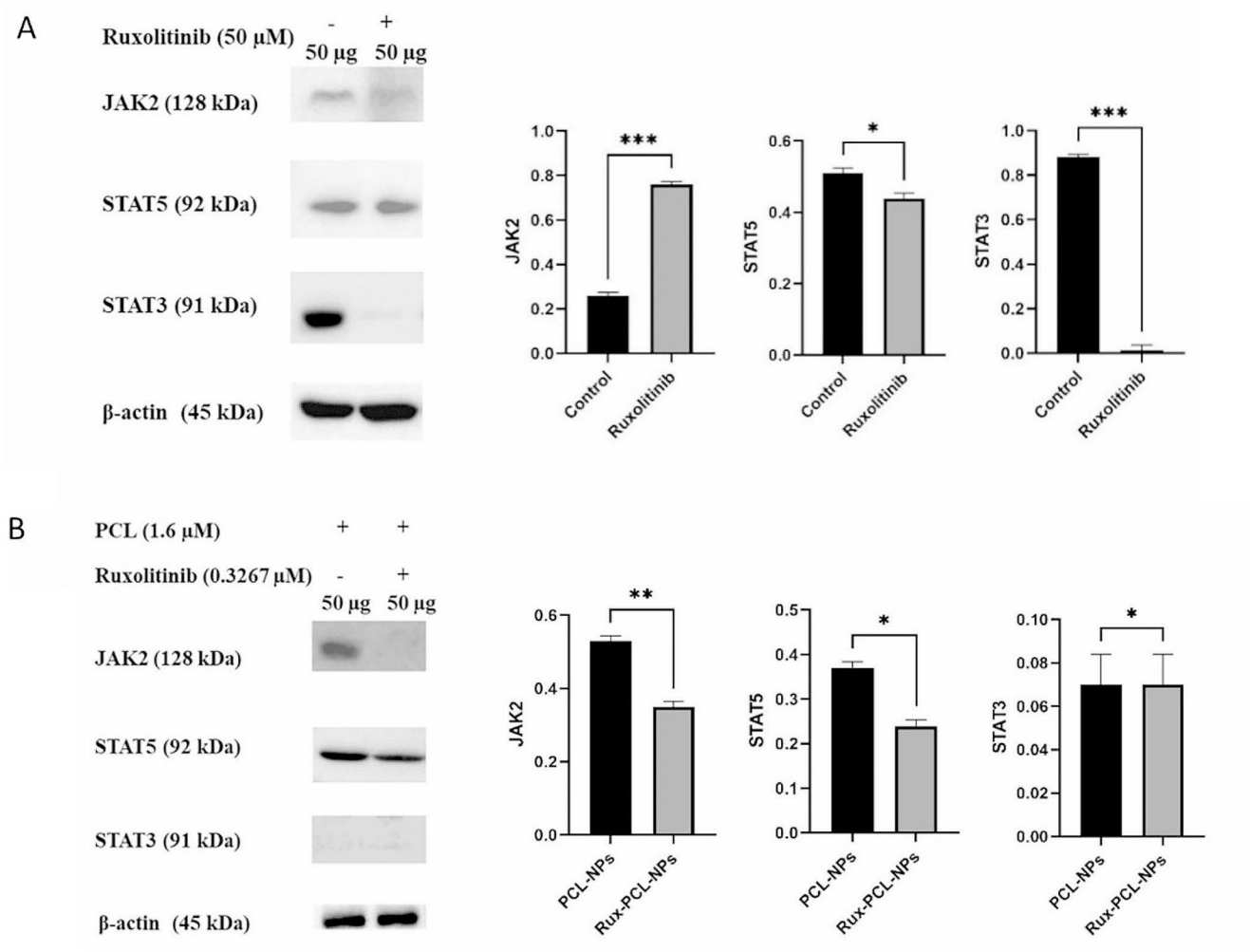

Fig. 6 Effects of ruxolitinib (**a**), PCL-NPs (**b**), and Rux-PCL-NPs (**b**) on JAK/STAT signaling. Total protein lysates (50 µg) of ruxolitinib (**a**), PCL-NPs (**b**), and Rux-PCL-NPs (**b**) were examined by western blotting

cell membrane surface is negatively charged [25]. Yue et al. demonstrated that the positive charge further increased the uptake of NPs into the cell [26]. Unal et al. determined that the interaction between NPs and the mucus layer was significantly increased by coating NPs with positively charged materials [27]. PCL has a negative surface charge due to its terminal carboxylic groups. Unal et al. determined that in uncoated NPs, the zeta potential ranged from −20.1 to -25.8, whereas in coated NPs, the surface charge ranged from +29.6 to +57. [10]. They demonstrated that the zeta potential of NPs coated with chitosan and PCL used in the study changed from negative to positive [10]. According to our results, the surface charge of the Rux-PCL-NPs increased from −44.6 to 0.471 mV (Table 1).

The degree of homogeneity of the formulation is indicated by the PDI. 0 indicates a monodisperse system, which indicates a heterogeneous system containing aggregates, polymer residues, and particles of varying sizes. Unal et al. demonstrated that the PDI values of paclitaxel-loaded PCL and chitosan nanoparticles were close to 0. According to our findings, the synthesized Rux-PCL-NPs were homogeneous since the PDI was close to 0 (Table 1).

A number of benefits can be achieved by loading bioactive drugs into nanoparticle systems, including increasing and prolonging their stability, improving therapeutic efficacy, allowing precise doses to be tailored to meet therapeutic needs, and minimizing the risk of degradation and nonspecific uptake by cells [28]. Studies have shown that the encapsulation efficiency of NPs prepared with high-molecular-weight (MW) PCL is greater than that of NPs coated with low-molecular-weight PCL [25, 29]. Increasing the organic phase viscosity may lead to a higher encapsulation efficiency. Unal et al. demonstrated that the encapsulation efficiency of NPs prepared with 80,000 MW PCL ranged from 59.4 to 64.7%, while that of NPs prepared with 14.000 MW PCL varied from 51.3 to 63.1%. In the

same study, they determined that the drug loading capacity of NPs prepared with 80.000 MW PCL was greater than that of NPs prepared with 14,000 MW PCL, with ranges of 6.2–8.4% and 5.2–6.6%, respectively. This suggests that the molecular weight of PCL can influence the amount of drug that can be loaded into the nanoparticles [10]. According to our findings, the %EE values of the Rux-PCL-NPs prepared with 66,000 MW PCL were 61% and 6.1%, respectively (Table 1). Moreover, the loading of ruxolitinib into PCL was effective due to the increase in the %EE values.

Unal et al. determined that the sizes of paclitaxel-loaded NPs prepared with 80,000 MW PCL were 238–380 nm and that the NP formulations were smooth and spherical [10]. According to our findings, the molecular size of ruxolitinib decreased as a result of its encapsulation with PCL, the size of the Rux-PCL-NPs varied between 97 and 101 nm, and all the NP formulations had smooth and spherical surfaces (Fig. 1a and b).

Unal et al. demonstrated the in vitro release profiles of PCX from PCL-NPs by the dialysis membrane technique. They determined that paclitaxel can be released from the PCL formulation for up to 96 h. They showed that a sudden release of paclitaxel from paclitaxel-loaded chitosan (CS) and paclitaxel-loaded poly-L-lysine (PLL) nanoparticles occurred in the first 24 h, and the release rate of paclitaxel may vary depending on the coating material [10]. In the same study, when looking at the rates of drug release according to particle size, they found that smaller-sized paclitaxel-loaded PCL nanoparticles showed a higher release rate and that larger-sized paclitaxel-loaded chitosan-coated PCL nanoparticles showed a slower release rate [10]. Kamaraj et al. determined that the release of DDA from 14-deoxy 11.12-didehydroandrographolide-loaded polycaprolactone nanoparticles (nanoDDA) was 20% in the first 24 h, increased up to 50% up to 192 h, and decreased at the 264th hour [30]. According to our findings, 51% of the ruxolitinib was released from PCL nanoparticles in the first 24 h, and 77% of the ruxolitinib was released at the end of the 96th hour. According to our results, the controlled release of the active ingredients of ruxolitinib from PCL nanoparticles can be achieved (Fig. 2).

Schneider et al. reported that ruxolitinib decreases proliferation in SKBR3, MCF-7, and MDA-MB-468 cells, and the IC_{50} values of ruxolitinib were 13.94 µM, 30.42 µM, and 10.87 µM, respectively [31]. Abamor et al. determined that the toxic effects of blank nanoparticles and quercetin-loaded PCL nanoparticles were quite low. They demonstrated that even at low concentrations, nanoparticles show similar cell viability to that of the control [11]. Ozturk et al. demonstrated that lower cell viability was obtained with 5-FU-loaded PCL NPs and that empty PCL nanoparticles had no effect on the viability of Caco-2 cells [13]. Boca et al. have demonstrated that ruxolitinib-conjugated-gold nanoparticles inhibit the proliferation of fibroblasts by inhibiting the JAK2 protein, compared to the treatment of ruxolitinib alone [5]. According to our results, PCL nanoparticles did not affect the viability of cells (Fig. 3c). In addition, our study indicated that the IC_{50} of ruxolitinib decreased from 50 µM to 0.3267 µM upon treatment with the ruxolitinib nanoformulation (Fig. 3a and b). Our study shows that Rux-PCL-NPs inhibits the proliferation of BT474 cells more effectively than the treatment of ruxolitinib alone (Fig. 4). According to our findings, similar results can be obtained with free ruxolitinib treatment by treating BT474 cells with lower doses of Rux-PCL-NPs.

Apoptosis is regulated by a series of events [32]. The loss of mitochondrial membrane potential activates the release of cytochrome C, located between the mitochondrial double membrane, into the cytoplasm, activates the mitochondrial pathway of apoptosis, and stimulates caspase activation [33]. Members of the protease caspase family play important roles in the initiation and execution of apoptosis [34]. Apoptosis is regulated by pro- and antiapoptotic members of the BCL-2 family [21]. The increased resistance of several types of cancer cells to chemotherapy is caused by the activation of MCL-1, BCL-XL, BCL-2, and BCL-W, which are antiapoptotic members of the BCL-2 family [35]. Li et al. determined that ruxolitinib treatment for 48 h increased the expression of cleaved PARP and Caspase-9, -8, and −3 in SW620 and LS411N colorectal cancer cells [36]. Bragta et al. demonstrated that carboplatin-loaded poly-(ε-caprolactone) nanoparticles (CBDCA-PCL-NPs) caused 57.6% of B16F1 melanoma cells to undergo apoptosis, and CBDCA-PCL-NPs-Gel caused 80.2% of B16F1 melanoma cells to undergo apoptosis [19]. They demonstrated that CBDCA-PCL-NPs-Gel treatment decreased Bcl-2 expression in tumor tissues by 2.5-fold and increased Bax expression by 2.03-fold in tumor tissues and B16F1 cells. Additionally, they determined that the nanoform of carboplatin can induce Caspase-8- and Caspase-3-mediated apoptosis in tumor tissues and B16F1 melanoma cells [19]. Bhattacharya demonstrated by an Annexin V assay that the percentage of apoptotic cells in NCI-H460 cells treated with free gefitinib, gefitinib PCL10.000NPs, gefitinib PCL45.000NPs, and gefitinib PCL80.000NPs increased by 30.78 ± 3.78%, 31.67 ± 3.67%, and 46.78 ± 4.56%, respectively [37]. According to our results, treatment of BT474 cells with ruxolitinib and Rux-PCL-NPs inhibited apoptosis, decreasing Caspase-8, Caspase-3, Mcl-1, and Bcl-2 expression (Fig. 5a, b, c and d).

JAK2 plays an essential role in regulating the proliferation and apoptosis of cancer cells by activating the STAT3/STAT5 and PI3K/AKT pathways [38]. STAT3 and STAT5 modulate the expression of genes involved in cell growth,

angiogenesis, and survival [39, 40]. Therefore, drug resistance and relapse may occur. Hyperactivation of STAT3 and STAT5 is caused by mutations in these genes and is associated with cancer progression in patients [41]. STAT3 activation occurs in all classes of breast cancer but is most common in TNBCs [42]. STAT5 stimulates both terminal differentiation of the mammary gland and survival [42]. STAT5 increases the expression of pro-survival genes, such as Bcl-Xl. STAT5 is constitutively active in hormone-responsive breast tumors [42]. Kim et al. demonstrated that the IL-6/STAT3/ROS pathway may be associated not only with breast cancer progression and inflammation but also with increased formation of breast cancer stem cells [35]. Pro- and antiapoptotic proteins such as Bak/Bax and Bcl-2 are also associated with the JAK/STAT signaling pathway. Boca et al. demonstrated that ruxolitinib coated with gold nanoparticles prevented fibroblast proliferation by blocking JAK2 expression in fibroblasts [5]. No study on ruxolitinib combined with another polymer has been reported in the literature. According to our findings, STAT5 and JAK2 expression decreased with Rux-PCL-NP treatment in BT474 cells, but there was no significant change in STAT3 expression (Fig. 6a and b).

Conclusions

In conclusion, the IC_{50} value of the ruxolitinib-loaded nanoparticles was reduced 50-fold compared with that of ruxolitinib. Additionally, Rux-PCL-NPs induced apoptosis by decreasing Caspase-8, Caspase-3, Bcl-2, Mcl-1, STAT5 and JAK2 expression. Rux-PCL-NPs can be a useful new therapeutic strategy for decreasing the toxicity of ruxolitinib and increasing its activity.

Abbreviations

ER	estrogen receptor
JAK	Janus kinase
NP	nanoparticle
PCL	poly-ε-caprolactone
PNP	polymeric nanoparticle
PR	progesterone receptor
Rux-PCL-NP	ruxolitinib-loaded nanoparticle
STAT	signal transducer and activator of transcription

Supplementary Information The online version contains supplementary material available at https://doi.org/10.1007/s11033-024-09764-3.

Acknowledgements The results shown in this paper were part of the Ph.D. thesis of Esin Guvenir Celik. BT474 cells were kindly donated by Professor Ayse Elif ERSON BENSAN and Assistant Professor Doctor Pelin Ozfiliz KILBAS for our doctorate research project. PCL was kindly donated by Associate Professor Umut KADIROGLU for our doctorate research project.

Author contributions The study conception and design were contributed by EGC and OE. Data collection, material preparation, and analysis were performed by EGC. This manuscript was written by EGC and OE, and EGC and OE approved the published version. EGC and OE read and approved the final manuscript.

Funding Part of this research was financially supported by the Research Projects Department of Bilecik Şeyh Edebali University [Project No. 2018-02]. BŞEÜ.01–01].

Data availability No datasets were generated or analysed during the current study.

Declarations

Ethics approval We declare that the research presented in this article used a commercially available cell line and did not involve human participants or animals.

Competing interests The authors declare no competing interests.

References

1. López-Mejía JA, Mantilla-Ollarves JC, Rocha-Zavaleta L (2023) Modulation of JAK-STAT signaling by LNK: a forgotten oncogenic pathway in hormone receptor-positive breast Cancer. Int J Mol Sci 24
2. Kharb R, Haider K, Neha K, Yar MS (2020) Aromatase inhibitors: role in postmenopausal breast cancer. Arch Pharm (Weinheim) 353
3. Stevens LE, Peluffo G, Qiu X et al (2023) JAK–STAT signaling in inflammatory breast Cancer enables chemotherapy-resistant Cell States. Cancer Res 83:264–284. https://doi.org/10.1158/0008-5472.CAN-22-0423
4. Stover DG, Gil Del Alcazar CR, Brock J et al (2018) Phase II study of ruxolitinib, a selective JAK1/2 inhibitor, in patients with metastatic triple-negative breast cancer. NPJ Breast Cancer 4:10
5. Boca S, Berce C, Jurj A et al (2017) Ruxolitinib-conjugated gold nanoparticles for topical administration: an alternative for treating alopecia? Med Hypotheses 109:42–45
6. Singh SK, Singh S Jr, Lillard JW, Singh R (2017) Drug delivery approaches for breast cancer. Int J Nanomed 12:6205–6218
7. Shafei A, El-Bakly W, Sobhy A et al (2017) A review on the efficacy and toxicity of different doxorubicin nanoparticles for targeted therapy in metastatic breast cancer. Biomed Pharmacotherapy 95:1209–1218
8. Jain V, Kumar H, Anod HV et al (2020) A review of nanotechnology-based approaches for breast cancer and triple- negative breast cancer. J Controlled Release 326:628–647
9. Sinha VR, Bansal K, Kaushik R et al (2004) Poly-ε-caprolactone microspheres and nanospheres: an overview. Int J Pharm 278:1–23
10. Ünal S, Doğan O, Aktaş Y (2022) Paclitaxel-loaded polycaprolactone nanoparticles for lung tumors; formulation, comprehensive in vitro characterization and release kinetic studies. Ankara Universitesi Eczacilik Fakultesi Dergisi 46:1008–1028
11. Abamor ES (2018) A new approach to the treatment of leishmaniasis: quercetin-loaded polycaprolactone nanoparticles. J Turkish Chem Soc Sect A: Chem 5:1071–1082

12. Mahmoud BS, McConville C (2021) Development and optimization of irinotecan-loaded pcl nanoparticles and their cytotoxicity against primary high-grade glioma cells. Pharmaceutics 13
13. Öztürk K, Mashal AR, Yegin BA, Çalış S (2017) Preparation and in vitro evaluation of 5-fluorouracil-loaded PCL nanoparticles for colon cancer treatment. Pharm Dev Technol 22:635–641
14. Javaid S, Ahmad NM, Mahmood A et al (2021) Cefotaxime loaded polycaprolactone based polymeric nanoparticles with antifouling properties for in-vitro drug release applications. Polym (Basel) 13
15. Kumar N, Chaurasia S, Patel RR et al (2016) Atorvastatin calcium loaded PCL nanoparticles: development, optimization, in vitro and in vivo assessments. RSC Adv 6:16520–16532
16. Naeimifar A, Ahmad Nasrollahi S, Akbari Javar H et al (2022) Designing a Topical Nanoliposomal Formulation of Ruxolitinib phosphate. Pharm Sci 29:75–83
17. Jesus S, Fragal EH, Rubira AF et al (2018) The inclusion of Chitosan in Poly-ε-caprolactone nanoparticles: Impact on the delivery system characteristics and on the Adsorbed Ovalbumin secondary structure. AAPS PharmSciTech 19:101–113
18. Bernabeu E, Helguera G, Legaspi MJ et al (2014) Paclitaxel-loaded PCL-TPGS nanoparticles: in vitro and in vivo performance compared with Abraxane®. Colloids Surf B Biointerfaces 113:43–50
19. Bragta P, Sidhu RK, Jyoti K et al (2018) Intratumoral administration of carboplatin bearing poly (ε-caprolactone) nanoparticles amalgamated with in situ gel tendered augmented drug delivery, cytotoxicity, and apoptosis in melanoma tumor. Colloids Surf B Biointerfaces 166:339–348
20. Civallero M, Cosenza M, Pozzi S, Sacchi S (2017) Ruxolitinib combined with vorinostat suppresses tumor growth and alters metabolic phenotype in hematological diseases. Oncotarget 8:103797–103814
21. Lim ST, Jeon YW, Gwak H et al (2018) Synergistic anticancer effects of ruxolitinib and calcitriol in estrogen receptor-positive, human epidermal growth factor receptor 2-positive breast cancer cells. Mol Med Rep 17:5581–5588
22. Igney FH, Krammer PH (2002) Death and anti-death: Tumour resistance to apoptosis. Nat Rev Cancer 2:277–288
23. Khanna P, Lee JS, Sereemaspun A et al (2018) GRAMD1B regulates cell migration in breast cancer cells through JAK/STAT and Akt signaling. Sci Rep 8:1–10
24. Yang W, Wang L, Mettenbrink EM et al (2021) Nanoparticle toxicology. Annu Rev Pharmacol Toxicol 61:269–289
25. Miladi K, Sfar S, Fessi H, Elaissari A (2015) Encapsulation of alendronate sodium by nanoprecipitation and double emulsion: from preparation to in vitro studies. Ind Crops Prod 72:24–33
26. Yue ZG, Wei W, Lv PP et al (2011) Surface charge affects cellular uptake and intracellular trafficking of chitosan-based nanoparticles. Biomacromolecules 12:2440–2446
27. Ünal H, D'Angelo I, Pagano E et al (2015) Core–shell hybrid nanocapsules for oral delivery of camptothecin: formulation development, in vitro and in vivo evaluation. J Nanopart Res 17
28. El Yousfi R, Brahmi M, Dalli M et al (2023) Recent advances in Nanoparticle Development for Drug Delivery: a Comprehensive Review of Polycaprolactone-based Multi-arm architectures. Polymers (Basel) 15
29. Ali R, Farah A, Binkhathlan Z (2017) Development and characterization of methoxy poly(ethylene oxide)-block-poly(ε-caprolactone) (PEO-b-PCL) micelles as vehicles for the solubilization and delivery of tacrolimus. Saudi Pharm J 25:258–265
30. Kamaraj N, Rajaguru PY, Issac P, kumar, Sundaresan S (2017) Fabrication, characterization, in vitro drug release and glucose uptake activity of 14-deoxy, 11, 12-didehydroandrographolide loaded polycaprolactone nanoparticles. Asian J Pharm Sci 12:353–362
31. Schneider J, Jeon YW, Suh YJ, Lim ST (2022) Effects of Ruxolitinib and Calcitriol Combination Treatment on various molecular subtypes of breast Cancer. Int J Mol Sci 23:2535
32. Çakir HK, Eroglu O (2021) In vitro anti-proliferative effect of capecitabine (Xeloda) combined with mocetinostat (MGCD0103) in 4T1 breast cancer cell line by immunoblotting. Iran J Basic Med Sci 9:1515–1522
33. Olson M, Kornbluth S (2005) Mitochondria in Apoptosis and Human Disease
34. Boice A, Bouchier-Hayes L (2020) Targeting apoptotic caspases in cancer. Biochim Biophys Acta Mol Cell Res 1867:118688
35. Kim JW, Gautam J, Kim JE et al (2019) Inhibition of tumor growth and angiogenesis of tamoxifen-resistant breast cancer cells by ruxolitinib, a selective JAK2 inhibitor. Oncol Lett 17:3981–3989
36. Hu X, Li J, Fu M et al (2021) The JAK / STAT signaling pathway: from bench to clinic. 6:402
37. Bhattacharya S (2022) Genotoxicity and in vitro investigation of Gefitinib-loaded polycaprolactone fabricated nanoparticles for anticancer activity against NCI-H460 cell lines. J Exp Nanosci 17:214–246
38. Ishida S, Akiyama H, Umezawa Y et al (2018) Mechanisms for mTORC1 activation and synergistic induction of apoptosis by ruxolitinib and BH3 mimetics or autophagy inhibitors in JAK2-V617F-expressing leukemic cells including newly established PVTL-2. Oncotarget 9:26834–26851
39. Yeh JE, Toniolo PA, Frank DA (2013) JAK2-STAT5 signaling. JAKSTAT 2:e24635
40. Celik EG, Eroglu O (2023) Combined treatment with ruxolitinib and MK-2206 inhibits the JAK2/ STAT5 and PI3K/AKT pathways via apoptosis in MDAMB-231 breast cancer cell line. Mol Biol Rep 50:319–329. https://doi.org/10.1007/s11033-022-08034-4
41. Orlova A, Wagner C, de Araujo ED et al (2019) Direct Targeting options for STAT3 and STAT5 in Cancer. Cancers (Basel) 11:1930
42. Walker SR, Xiang M, Frank DA (2014) Distinct roles of STAT3 and STAT5 in the pathogenesis and targeted therapy of breast cancer. Mol Cell Endocrinol 382